Magnetic Resonance Imaging of Core Flooding in a Metal Core Holder

Ming Li[1,2], Dan Xiao[1], Mojtaba Shakerian[1,3], Armin Afrough[1,2], Fred Goora[1]
Florin Marica[1], Laura Romero-Zerón[2], Bruce Balcom[1]
[1]UNB MRI Research Centre, Department of Physics, University of New Brunswick, Canada; [2]Chemical Engineering Department, University of New Brunswick, Canada;
[3]Mechanical Engineering Department, University of New Brunswick, Canada

This paper was prepared for presentation at the International Symposium of the Society of Core Analysts held in Snowmass, Colorado, USA, 21-26 August 2016

ABSTRACT

Magnetic Resonance (MR) is widely employed in the petroleum industry for down-hole logging and for laboratory core analysis. Sensitivity of the magnetic resonance experiment to fluid type and fluid environment makes it uniquely well suited to these applications. The same advantages should accrue to Magnetic Resonance Imaging (MRI) measurements of core flooding experiments. The ability of MRI to directly measure fluid saturation and fluid environment in three dimensions as a function of time has, to this point, not been fully realized for core flood applications. In this paper we describe the development of a series of technologies, which have overcome the traditional limitations.

Challenges include the necessity of methods that are in the first instance quantitative for fluid saturation, and methods that permit the determination of the spatially resolved T_2 distribution. Putative methods must be high sensitivity and methods must be translated to high pressure, high temperature core holders.

We have developed a new generation of non-magnetic metallic core holders, (Hastelloy based) which permit MRI measurements at 5000 psi and temperatures above 100 °C. The Radio Frequency (RF) probe is located inside the metal case to increase the experimental Signal to Noise Ratio (SNR). MRI requires the application of precise rapidly switched magnetic field gradients to encode position and motion in the MR signal. The presence of substantial metal in the sample space ordinarily degrades magnetic field gradient performance. However, the high resistivity of Hastelloy and related alloys results in short lived eddy currents, which do not significantly impair gradient switching. We have developed experimental methods to measure and correct magnetic field gradient waveforms to ensure near ideal gradient performance, even in the presence of a metal core holder.

Previously developed pure phase encode MRI measurements permitted saturation determination and T_2 mapping at low magnetic field strength (8.5 MHz for ^{1}H) but the insensitivity of these methods limited routine core flood imaging to 1D.

Fast and accurately switched magnetic field gradients now permit the introduction of fast frequency encoding MRI methods that are quantitative even for short T_2 populations (a few msec). These new methods permit 3D MRI of core plug samples in low field MRI instruments that are common in the industry. 3D imaging of core plugs, with 1.5" diameter and lengths of several inches, is possible with imaging times on the order of 10 minutes, in magnets of this type. This is sufficiently fast to permit time resolution of core flooding measurements. Recent examples of polymer flooding and supercritical CO_2 flooding in Berea core plugs illustrate these experimental advantages.

INTRODUCTION

Magnetic Resonance (MR) and Magnetic Resonance Imaging (MRI) have been widely employed for rock core and petroleum studies in both industry and academic laboratories [1-7]. These techniques provide a wealth of information on reservoir and fluid behavior including fluid viscosity, fluid type, fluid saturation, rock wettability, permeability, capillary pressure and pore size distributions [1, 8].

Low pressure MR compatible core holders have been employed for core flooding studies [9], but realistic studies require core holders that will function at temperatures and pressures that represent reservoir conditions. Commercial MR/MRI compatible core holders are available from several vendors. Core holders based on polymer composite materials have been available for many years. More recently core holders based on ceramic and zirconia materials have become available. In most cases these core holders fit inside an existing RF probe which of necessity will be displaced from the sample by the core holder body. MR/MRI is unfortunately an insensitive technique. High static magnetic field increases the experimental sensitivity however magnetic susceptibility effects in the pore space generally limit the static field strength B_0 to less than 0.5 Tesla (21 MHz for ^{1}H) for MRI and to 0.05 Tesla (2 MHz for ^{1}H) for MR relaxation time distribution measurements in reservoir core plugs [1,7].

The simplest way to increase the sensitivity of the MR/MRI experiment for core analysis and core flooding, at fixed static field B_0, is to ensure the RF probe, which excites and detects the experimental signal, is located in close proximity to the sample. The principle of reciprocity [10] states that the sensitivity of the RF probe for detection is directly proportional to the radio frequency (RF) B_1 field in the sample space, per unit current in the RF probe, during excitation. Close proximity of the RF probe windings to the sample, according to the Biot Savart law, results in optimal sensitivity. Translated to a core holder design this means the RF probe should be integrated into the core holder, not positioned outside the core holder.

We have developed several generations of non-magnetic metal pressure vessels that are compatible with MR/MRI [11-13]. These vessels, which may be core holders, are typically non-magnetic, high strength, super alloys. Since the metal is an RF shield at the MR frequencies employed, the RF probe is positioned on the inside of the metal case in close proximity to the core plug [11-13]. Green Imaging Technologies and Oxford

Instruments have similarly incorporated an RF probe into their ceramic based core holder [14]. Proximity of sample and RF probe is very advantageous in terms of experiment sensitivity according to the principle of reciprocity as outlined above. Thermal conductivity of the metal case means that it is possible to temperature control the core holder by circulating water through a vessel in contact with the outer case of the core holder.

High quality MRI measurements require precise rapidly switched magnetic field gradients, despite the presence of metal structures, which may support eddy currents. A magnetic field gradient waveform correction technique has been employed in this work to correct the magnetic field gradient waveform, and ensure rapid gradient switching [15].

The pure phase encode MRI method, Single Point Ramped Imaging with T_1 Enhancement (SPRITE), has been widely employed to study fluids in porous media with relatively short relaxation lifetimes (typically hundreds μsec of T_2^*) [16]. SPRITE is very quantitative for fluid saturation measurements in rock core plugs. At low static magnetic fields, SPRITE is usually limited to 1D and 2D image measurements due to low sensitivity [13, 16]. SPRITE is however inherently immune to eddy currents and poor gradient waveforms [16]. 3D SPRITE images in previous work have been generally measured at high magnetic field [17, 18], for example 2.4 Tesla.

Spin Echo Single Point Imaging (SE-SPI) is a pure phase encode MRI technique [16]. T_2 mapping SE-SPI provides spatially resolved T_2 distributions which measure the fluid occupied pore size distribution and may reveal changes in fluid interaction with the pore surface [1, 9, 19]. Measurement of short lifetime T_2s requires rapid, precise gradient switching. SE-SPI is limited to 1D imaging due to low sensitivity.

Most MRI studies of rock core flooding are limited to 1D and 2D because a lengthy measurement time for 3D measurements at low magnetic field can hinder monitoring the displacement. 1D and 2D images may not accurately reflect the oil and water distribution in heterogeneous rock cores. Fast Spin Echo (FSE) imaging methods have been applied to investigate the 3D fluid content in core-plugs [1]. Conventional FSE employs a high gradient duty cycle and band selective RF pulses which limit the minimum echo time. Xiao [20] demonstrated that π-EPI provided superior quality 3D images of water content in rock core plugs compared to the FSE method at 2.4 Tesla (100 MHz for ^{1}H). Li [21] demonstrated the ability of the modified π-EPI MRI measurement to undertake fast 3D imaging of oil saturation distribution at low magnetic field, 0.2 Tesla (8.5 MHz for ^{1}H), with a low pressure core holder, during oil displacement processes. π -EPI MRI measurements generate high quality 3D images, which reflect the oil saturation distribution in rock cores.

In this work we show the integration of a high strength Hastelloy based metal core holder with two core flooding experiments. In the first experiment we undertake rapid 3D π-EPI imaging of saturation evolution, during water flooding and polymer flooding at high

pressure and ambient temperature. In the second experiment we employ 1D SPRITE imaging of oil saturation and SE-SPI T_2 mapping during supercritical CO_2 flooding, with temperature control at high pressure. SPRITE MRI measures the macroscopic evolution of oil saturation in the core plug, as does SE-SPI T_2 mapping. The T_2 mapping experiment however also reports on pore scale changes in fluid behaviour, all spatially and temporally resolved.

CORE HOLDER AND MRI INSTRUMENTATION

The MR/MRI compatible core holder employed in these studies was a prototype non-magnetic core holder fabricated from Hastelloy-C276 metal. Hastelloy is commonly employed in the petroleum industry. It features a high yield strength, 360 MPa, and low electrical conductivity, 0.76×10^6 S/m. Polymer components of the core holder were fabricated from high strength PEEK, which features very low background MR signal.

The core holder is designed for a maximum confining pressure of 5000 psi, with a safety factor of 3.5. The maximum design operating temperature is 135 °C. The core holder has been pressure tested to 5000 psi. The core holder, illustrated in Figure 1, will hold core plugs, 1.5" in diameter with a typical length of 2". The Hastelloy core holder is 14.8" in length with an outside diameter of 3.5". A metallic MR/MRI compatible core holder is conceptually appealing given the long history of metal core holders in the industry. With the RF probe situated inside the metal case, the RF shield for the RF probe is the core holder itself. Reduced noise and increased signal due to the principle of reciprocity [10] in this style core holder can improve the experimental SNR by at least a factor of 2 [11]. The RF probe in the core holder is tuned and matched with an external tuning circuit.

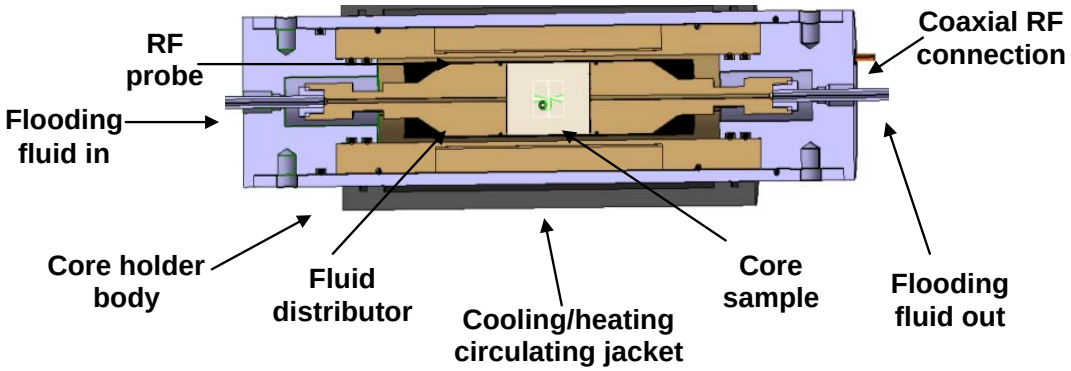

Figure 1. Cross-sectional diagram of a Hastelloy based core holder, employed for MR and MRI monitoring of core flooding processes at reservoir temperature and pressure. The RF probe is inside the metal case, in close proximity to the core plug sample. The plane displayed does not show external connection to the confining fluid.

The cylindrical geometry of the core holder ensures that the static B_0 field homogeneity is not distorted in the sample space [11], despite the use of a metal vessel. Switched magnetic field gradients will induce eddy currents in the metal structure of the core holder. The symmetry of the core holder ensures these eddy currents generate secondary

magnetic field gradients, which cause a temporal distortion of the magnetic field gradient waveform in the sample space.

We have recently developed methods to measure and correct the magnetic field gradient waveform [15]. Figure 2 (a) shows a magnetic field gradient measured in the presence of a Nitronic metal core holder. Figure 2 (b) shows the corrected waveform, switched to twice the amplitude. The waveform of Figure 2 (b) has an ideal trapezoidal shape with a rise time (10% to 90% level) of less than 100 µsec, a factor of 4 reduced from the original waveform. Rapid, accurate, gradient switching is critical for fast frequency encoding MRI methods such as π-EPI as employed in this work. They are also vital to observe short T_2 signal components (a few msec) in T_2 mapping SE-SPI measurements.

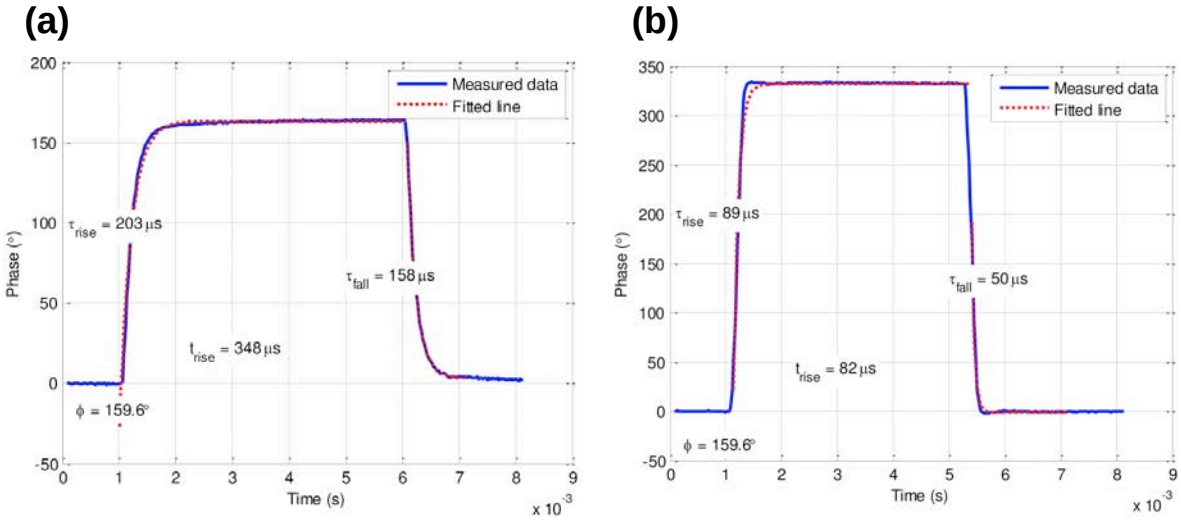

Figure 2. Magnetic field gradient waveforms measured in the presence of a Nitronic metal core holder. The figures plot signal phase, which is directly proportional to the instantaneous gradient amplitude. (a) Gradient waveform, maximum amplitude 3.1 Gauss/cm, before correction. (b) Gradient waveform, maximum amplitude 6.2 Gauss/cm, after correction. Time constants τ characterize an exponential fit. The t_{rise} is the time for 10% to 90% switch.

The low electrical conductivity of the Hastelloy core holder greatly simplifies gradient waveform correction. Although significant eddy currents are induced, they decay rapidly. The waveforms of Figure 2, as with Hastelloy results, are similar to those observed in the absence of a metal core holder. Other metal structures in the magnet, with higher conductivity, dominate the long time constant eddy current behaviour.

A Quizix precision pump QX-6000SS (Chandler Engineering, Broken Arrow, OK) and an ISCO pump (Teledyne ISCO, Lincoln, NE) were employed for fluid injection. MR/MRI measurements were performed on a 0.2 Tesla Maran DRX permanent magnet spectrometer (Oxford Instruments, Abingdon, Oxon, UK). A Tomco 3445 RF amplifier (Tomco Technologies, Stepney, SA, Australia) powered a homemade solenoid RF probe, with 1.75 inch inside diameter. The 3D gradient coil was driven by an AE Techron 7782 gradient amplifier (AE Techron, Elkhart, IN), providing maximum gradient strengths of

26, 24 and 33 Gauss/cm in the X, Y and Z directions, respectively. Figure 3 shows the schematic orientation of a 3D core plug in the magnet.

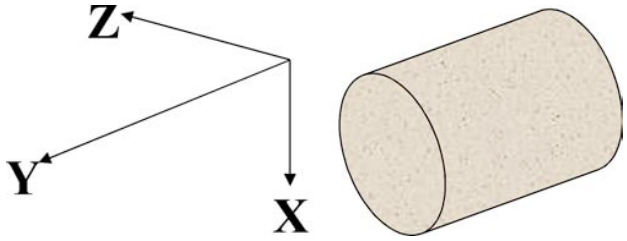

Figure 3. Schematic showing orientation of a core plug in the magnet. X, Y, and Z are the magnetic field gradient orientations.

Two home built programs, Unisort and Acciss, written in the IDL environment (Exelis VIS, CO, USA), were employed to reconstruct the SPRITE MRI images. Another home built program, written in MATLAB (MathWorks, Natick, MA, USA), was employed to reconstruct the 3D π-EPI images.

FLUIDS, ROCK CORE PLUGS AND FLOODING EXPERIMENTS

MRI Monitoring Polymer Flooding

A viscosity standard S6 oil (Cannon Instrument Company, State College, PA) was employed as the oil phase. The S6 oil viscosity and density were 10 cP and 0.88 g/cm^3 at 20 °C, respectively. H_2O brine, 1 wt% NaCl, was employed to determine the sample pore volume. D_2O (99.9 %, CDN Isotopes Inc., Pointe-Claire, QC, Canada) brine, 1 wt% NaCl, was employed to distinguish oil and water phases in the cores during MRI measurements. Alcoflood 935 polymer (Ciba Specialty Canada Inc., Mississauga, ON, Canada) was diluted to a concentration of 0.6 wt% in D_2O brine for polymer flooding. The viscosity of the polymer solution was 101 cP at a shear rate of 7 s^{-1} [21]. A Berea core plug (Kocurek Industries, TX, USA) was employed. Length was 5.2 cm, diameter 3.8 cm and pore volume 11.3 cm^3 with a porosity of 19 % and an absolute permeability of 74 mD.

The Berea core plug was dried at 100 °C to a constant weight and then saturated with 1 wt% NaCl H_2O brine. The pore volume of the core plug was calculated gravimetrically. The absolute permeability of the two samples was determined based on Darcy's law.

D_2O brine was employed to displace H_2O brine. 1D double half k SPRITE MRI measurements commenced simultaneously to monitor this displacement. D_2O injection ceased when the 1D SPRITE MRI profile intensity was constant. After displacement of H_2O brine with D_2O brine, approximately 10 PV S6 oil was injected into sample to displace D_2O brine. Further 1D SPRITE MRI measurements monitored this displacement. No further water production was observed and the 1D SPRITE MRI profile intensity was constant after sufficient oil was injected into the core plug.

A confining fluid pressure of 1000 psi was provided by compressed nitrogen gas. The back pressure regulator was set at 700 psi. Water flooding and polymer flooding were undertaken at ambient temperature. The flow rate of D_2O water flooding and polymer flooding was 0.04 ml/min. Water flooding was switched to polymer flooding when no additional oil production resulted from water flooding.

3D π-EPI measurements were undertaken to monitor the progression of flooding. The π-EPI measurement required 32 signal averages with a total imaging time of 16 minutes. The nominal image resolution was 1.4 mm with an echo time of 3 msec.

MRI Monitoring Supercritical CO_2 Flooding

Liquid CO_2 was employed to displace air in a Berea core plug, similar to the one described above for polymer flooding measurements. Decane was injected at high flow rate and high pressure to displace the liquid CO_2 in the sample. Supercritical CO_2 flooding commenced, with a flow rate 0.04 ml/min, and an injection pressure of 1300 psi and similar back pressure, at 40 °C with a confining pressure of 1500 psi. Bulk free induction decay, bulk CPMG and SPRITE centric scan measurements monitored the flooding. SE-SPI T_2 distribution mapping was undertaken as well to monitor flooding. 1D DHK SPRITE measurements, 64 signal averages, required 10 minutes per image with a nominal resolution 1.6 mm. SE-SPI T_2 mapping measurements employed 1536 echoes with 4 signal averages for a total imaging time of 29 minutes and a nominal image resolution of 1.1 mm. The echo time was 1.8 msec for all echoes.

RESULTS AND DISCUSSION

Figure 4 shows a series of 2D oil saturation images extracted from 3D π-EPI images in three orientations during water flooding and polymer flooding in a Berea core plug. The π-EPI image acquisition was undertaken with parameters that ensure a saturation weighted image. Image calibration with a reference sample permits absolute quantification of saturation as shown in Figure 4. The average initial oil saturation was 0.68 in the core plug.

Water flooding displaced oil in a piston-like displacement to an average residual oil saturation of 0.42. The piston like displacement is due to a favourable mobility ratio. Polymer flooding decreased oil saturation from 0.42 to 0.38, improving the oil recovery by 5.9 % OOIP. High intensity oil signal was observed in the tubing and at the interface of the PEEK distributor and the core plug. Only the image intensity in the core plug region was considered when calculating oil saturation and oil recovery.

The π-EPI measurement time, 16 minutes, is for single images. The temporal resolution for monitoring flooding processes can be improved by a factor equal to the number of interleaves in the data acquisition, in this case 8. This increases the temporal resolution from 16 minutes to 2 minutes, with simple view sharing [21, 22]. Temporal resolution this fine permits very dramatic 3D animations of the flooding process.

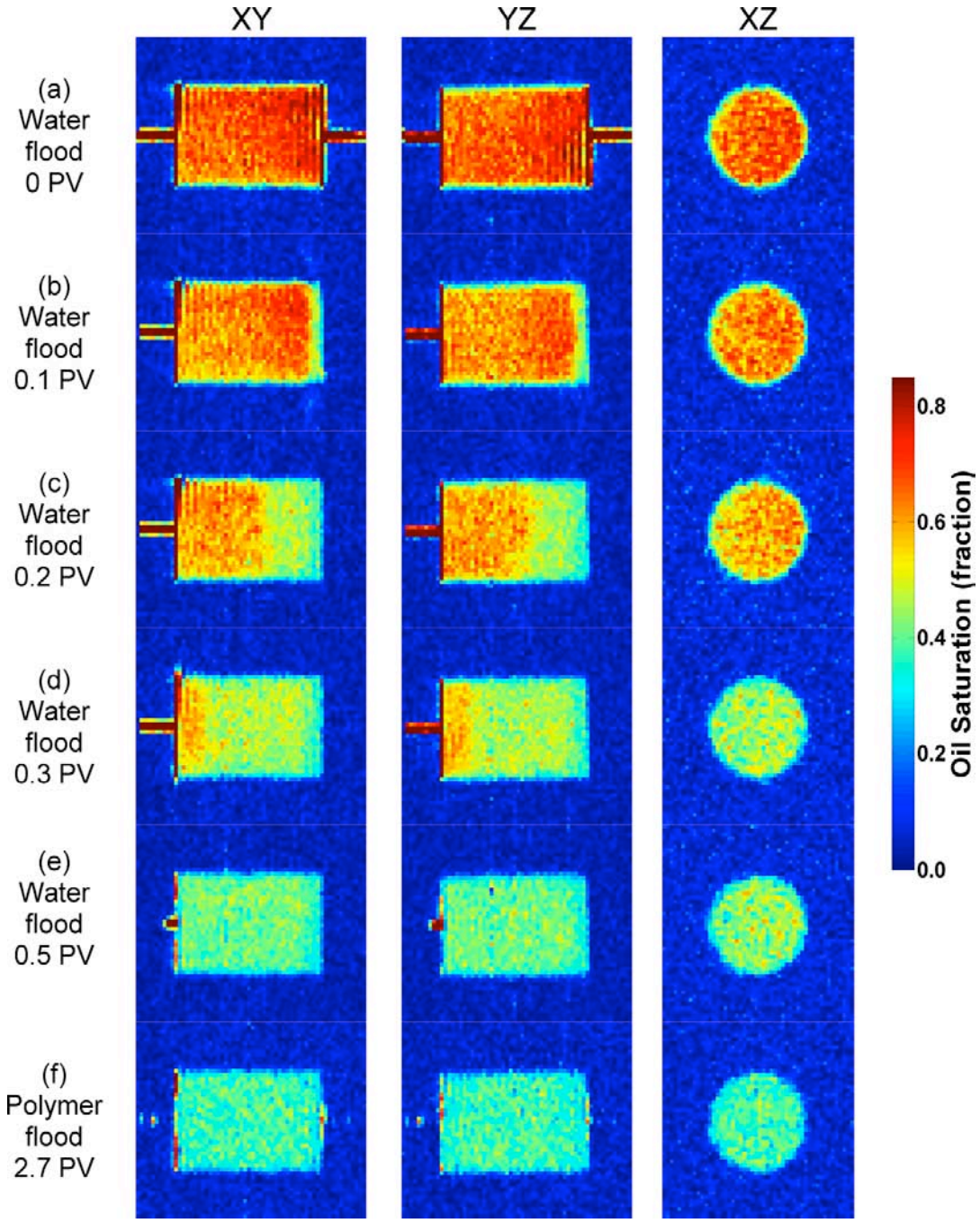

Figure 4. 2D oil saturation images extracted from 3D π-EPI images in three orientations during water flooding and polymer flooding in a Berea core plug. X, Y and Z directions were defined in Figure 3. The flooding is from right to left in the XY and YZ slices. The average initial oil saturation was 0.68 in the core plug (a). Water flooding displaced the oil in a piston-like displacement (b-e) to a residual oil saturation of 0.42. Polymer flooding decreased oil saturation from 0.42 to 0.38, improving the oil recovery by 5.9 % OOIP.

Figure 5 shows the oil recovery and pump injection pressure during water flooding and polymer flooding. The injection pressure for constant flow rate increased with polymer flooding as expected.

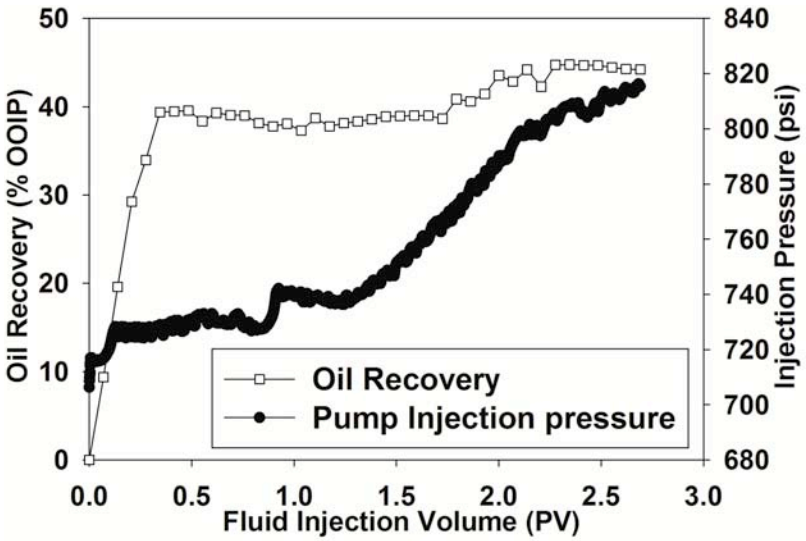

Figure 5. Oil recovery and pump injection pressure during water flooding and polymer flooding. Polymer flooding commenced at 0.8 PV. The back pressure regulator was set to 700 psi. Recovery was estimated based on the average π-EPI signal from the Berea core plug. Polymer flooding improved oil recovery by 5.9 % OOIP.

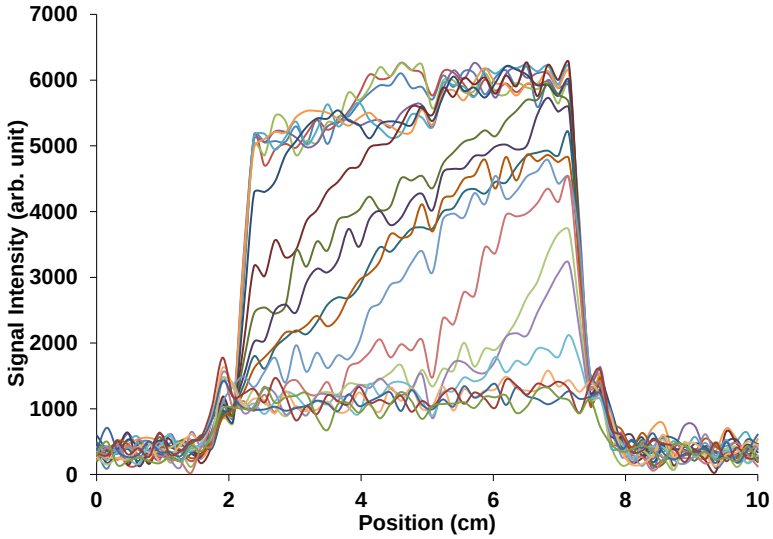

Figure 6. Time-resolved SPRITE imaging during supercritical CO_2 flooding to displace decane in a Berea core plug. Flooding is from left to right in the profiles. Oil signal gradually decreased during CO_2 flooding. The signal intensity is directly proportional to oil saturation. The overall experiment duration was approximately 29 hours.

Figure 6 shows double half *k* SPRITE images [16] of oil signal intensity along a Berea core plug during supercritical CO_2 flooding to displace decane. The oil signal intensity is

proportional to oil saturation as SPRITE is a very quantitative methodology. An inhomogeneous initial oil saturation was observed. A non-piston like displacement was apparent. CO_2 broke through to the outlet end of the core plug after the first few profiles. The majority of oil was recovered after CO_2 breakthrough.

Figure 7 shows the spatially resolved T_2 distribution along the Berea core plug at different stages of supercritical CO_2 flooding. At 0 hours of flooding the peak T_2 was approximately 90 msec throughout the core plug. A short T_2 lifetime peak of approximately 2 msec became more visible during flooding. The sub figures corresponding to 7.5 and 19.3 hours of flooding reveal a shift in the peak T_2 to shorter lifetimes near the flooding front. The decane oil recovery is almost 100 % OOIP due to the very low interfacial tension between liquid CO_2 and oil.

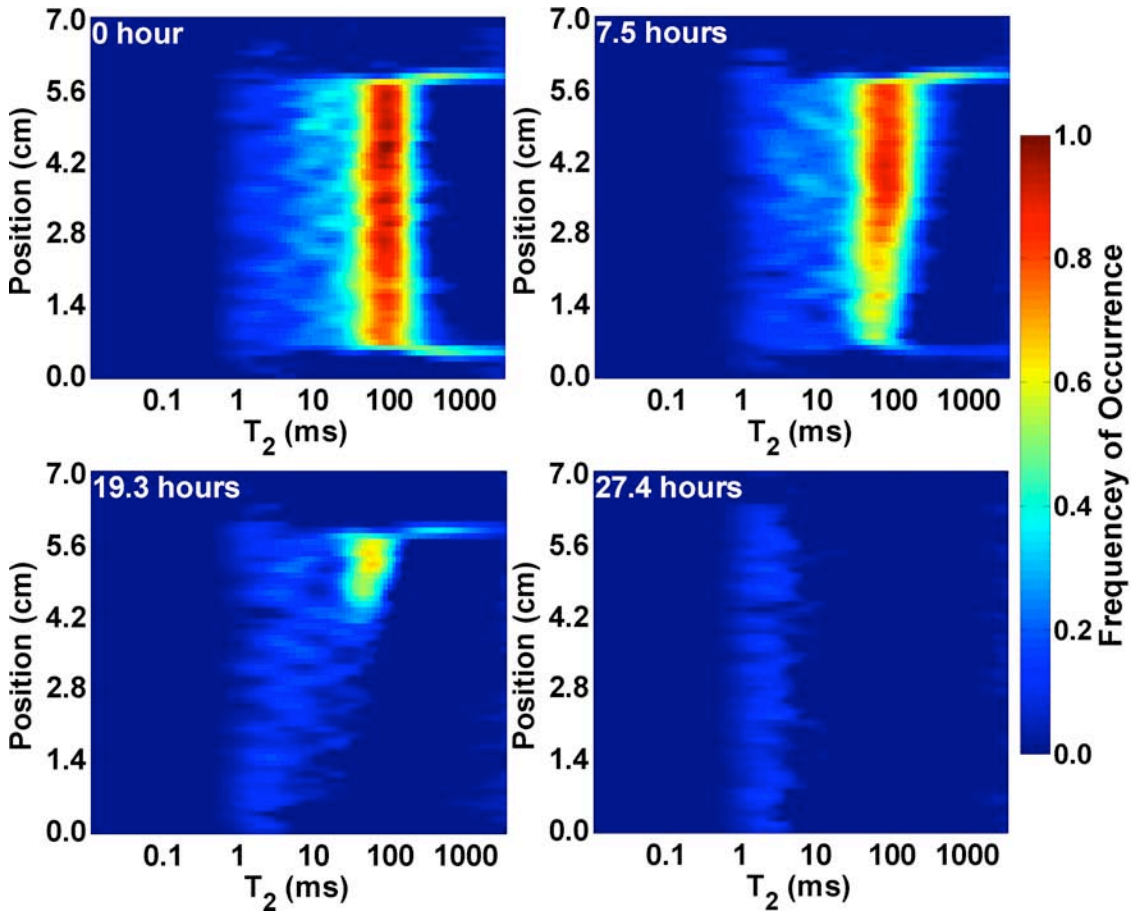

Figure 7. Spatially resolved T_2 distribution along the Berea core plug at different stages of supercritical CO_2 flooding to displace decane. The T_2 distribution was determined by Inverse Laplace transformation of the SE-SPI measurement data. The short lifetime, spatially uniform, T_2 distribution at 27.4 hours is consistent with the baseline image intensity in Figure 6 at long experimental flooding times. The overall experiment duration was approximately 29 hours.

CONCLUSION

A non-magnetic, metallic core holder (Hastelloy based) was employed for low field, 0.2 Tesla (8.5 MHz for ^{1}H) core flooding at representative reservoir pressure and temperature. The RF probe, integral to the core holder, increases experiment sensitivity. Magnetic field gradient waveform correction was undertaken to ensure rapid gradient switching. This permitted fast 3D frequency encode imaging with π-EPI and successful observation of short T_2 lifetime signal components in T_2 mapping SE SPI.

3D π-EPI MRI was employed to monitor the water flooding and polymer flooding in a Berea core plug housed in the Hastelloy core holder. High quality 3D oil saturation images were acquired. Pure phase encoding SPRITE and SE-SPI measurements were undertaken to monitor supercritical CO_2 flooding in a Berea core plug. Oil saturation profiles and the spatially resolved T_2 distribution were acquired during CO_2 flooding.

ACKNOWLEDGEMENTS

BJB thanks NSERC of Canada for a Discovery grant and the Canada Chairs program for a Research Chair in MRI of Materials. The authors also thank Green Imaging Technologies, Conoco Phillips, Saudi Aramco and the Atlantic Innovation Fund for financial support.

REFERENCES

1. J. Mitchell, T.C. Chandrasekera, D.J. Holland, F.L. Gladden, E.J. Fordham. Magnetic Resonance Imaging in Laboratory Petrophysical Core Analysis, Phys. Rep. 526 (2013) 165-225.
2. R. Freedman. Advances in NMR Logging, J. Pet. Technol. 58 (2006) 60-66.
3. A. Brautaset, G. Ersland, A. Graue, J. Stevens, J. Howard. Using MRI to Study in-situ Oil Recovery during CO_2 Injection in Carbonates. Paper SCA2008-41, International Symposium of the Society of Core Analysts, Abu Dhabi, UAE, Oct. 29-Nov. 2, 2008.
4. D. Green, J. Dick, M. McAloon, P.F. de J. Cano-Barrita, J. Burger, B. Balcom. Oil/Water Imbibition and Drainage Capillary Pressure Determined by MRI on a Wide Sampling of Rocks. Paper SCA2008-01, International Symposium of the Society of Core Analysts, Abu Dhabi, UAE, Oct. 29-Nov. 2, 2008.
5. D. Green, D. Veselinovic, B.J. Balcom, F. Marica. Applications of a New Technique to Acquire Spatially Resolved NMR Petrophysical Data. Paper SCA2012-32 , International Symposium of the Society of Core Analysts, Aberdeen, Scotland, UK, Aug. 27-30, 2012.
6. Y. Zhao, Y. Song, Y. Liu, H. Liang, B. Dou. Visualization and Measurement of CO_2 Flooding in Porous Media using MRI, Ind. Eng. Chem. Res. 50 (2011) 4707-4715.
7. J. Mitchell. Magnetic Resonance Core Analysis at 0.3 T. Paper SCA2014-010, International Symposium of the Society of Core Analysts, Avignon, France, Sept. 8-11, 2014.

8. G.R. Coates, L. Xiao, M.G. Prammer. NMR Logging Principles and Applications; Halliburton Energy Services: Houston, USA, 1999.
9. M. Li, D. Xiao, L. Romero-Zerón, B.J. Balcom. Monitoring Oil Displacement Processes with *k*-t Accelerated Spin Echo SPI, Magn. Reson. Chem. 54 (2016) 197-204.
10. D.I. Hoult. The Principle of Reciprocity in Signal Strength Calculations-a Mathematical Guide, Concepts Magn. Reson. 12 (2000) 173–187.
11. H. Han, M. Ouellette, B. MacMillan, F. Goora, R. MacGregor, D. Green, B.J. Balcom. High Pressure Magnetic Resonance Imaging with Metallic Vessels, J. Magn. Reson. 213 (2011) 90-97.
12. M. Ouellette, H. Han, B. MacMillan, F. Goora, R. MacGregor, M. Hassan, B.J. Balcom. Design of a Magnetic Resonance Imaging Compatible Metallic Pressure Vessel, J. Pressure Vessel Technol. 135 (2013) 045001-1-045001-7.
13. M. Ouellette, M. Li, G. Liao, E.M.A Hussein, L. Romero-Zerón, B.J. Balcom. Rock Core Analysis: Metallic Core Holders for Magnetic Resonance Imaging Under Reservoir Conditions, in: M. Johns (ed), Mobile NMR and MRI - Developments and Applications, New Developments in NMR; Royal Society of Chemistry, 2016, pp. 290-309.
14. Green Imaging Technologies Inc. P5 Cells for Overburden Studies, Fredericton, NB, Canada, 2015.
15. F.G. Goora, B.G. Colpitts, B.J. Balcom. Arbitrary Magnetic Field Gradient Waveform Correction Using an Impulse Response Based Pre-equlization Technique, J. Magn. Reson. 238 (2014) 70-76.
16. C.E. Muir, B.J. Balcom. Pure Phase Encode Magnetic Resonance Imaging of Fluids in Porous Media, Annu. Rep. NMR Spectrosc. 77 (2012) Burlington: Academic Press, 81-113.
17. Q. Chen, F. Rack, B.J. Balcom. Quantitative Magnetic Resonance Imaging Methods for Core Analysis, in: R.G. Rothwell RG (ed), New Techniques in Sediment Core Analysis, London, 2006, pp. 193-207.
18. L. Romero-Zerón, S. Ongsurakul, L. Li, B.J. Balcom. Visualization of the Effect of Porous Media Wettability on Polymer Flooding Performance through Unconsolidated Porous Media Using Magnetic Resonance Imaging, Pet. Sci. Technol. 28 (2010) 52-67.
19. O. Petrov, G. Ersland, B.J. Balcom. T_2 Distribution Mapping Profiles with Phase Encode MRI, J. Magn. Reson. 209 (2011) 39-46.
20. D. Xiao, B.J. Balcom. π Echo-planar Imaging with Concomitant Field Compensation for Porous Media MRI, J. Magn. Reson. 260 (2015) 38-45.
21. M. Li, D. Xiao, L. Romero-Zerón, F. Marica, B. MacMillan, B.J. Balcom. Mapping Three-Dimensional Oil Distribution with π-EPI MRI Measurements at Low Magnetic Field, J. Magn. Reson. 269 (2016) 13-23.
22. V. Rasche, R.W. de Boer, D. Holz, R. Proksa. Continuous Radial Data Acquisition for Dynamic MRI, Magn. Reson. Med. 34 (1995) 754-761.